17 May 1985, Volume 228, Number 4701 SCIENCE

Positron Emission Tomography: Human Brain Function and Biochemistry

Michael E. Phelps and John C. Mazziotta

Summary. Positron emission tomography (PET) is an analytical imaging technique that provides a way of making in vivo measurements of the anatomical distribution and rates of specific biochemical reactions. This ability of PET to measure and image dynamic biochemistry builds a bridge between the basic and clinical neurosciences founded on the commonality of the types of measurements made. Clinical findings with PET in humans are suggesting hypotheses that can be tested rigorously in the basic science laboratory.

The study of human brain function and its alterations with disease remains one of the most challenging and intriguing scientific issues of our time. Advances in brain research are increasing our understanding of the biochemical nature of the brain and are demonstrating that the earliest and most specific changes occurring in diseases of the brain are those that disturb its underlying biochemical processes. Until recently, we have had little direct access to the local biochemistry of the living human brain. Inferences about the chemical status of the brain are typically made by chemical assays of blood, cerebrospinal fluid, and urine or occasionally through biopsy procedures. With the development of positron-emission tomography or PET (*1*) these disturbances, along with the study of normal cerebral function can be investigated in humans (*2, 3*).

Knowledge concerning the biochemical basis of human disease should aid in developing earlier (when containment or reversibility of disease is more probable), more specific, and improved therapies. Therapeutic interventions for human brain disorders attempt to remove, block, or supplement chemical processes of the brain that have been altered by disease. For example, surgical therapies can resupply nutrients to deprived tissue by revascularization or can remove altered processes by tissue resection. Drug therapies are targeted at chemical reaction sequences that have been perturbed by disease, resulting in altered mood states and neurological dysfunction. In addition, local determinations of biochemical processes could provide more objective evaluations of therapeutic responses, better prognostic indicators, and improved differential diagnoses of diseases that are clinically homogeneous yet have diverse chemical alterations.

Equally important to the study of human diseases of the brain is the need to develop a better understanding of the structure, organization, and chemical basis of normal cerebral function. Although there is a rapid growth of knowledge occurring in this area from animal, isolated cell, and biochemical environments, corresponding direct investigations of the living human subject are needed. This, in part, results from the fact that there are anatomical areas and physiological functions found only in the human brain. In addition, identifying and treating diseases of the human brain require a better understanding of its normal processes. New scientific techniques such as PET provide one means to combine basic and clinical research to achieve these goals.

The PET Method

The use of PET to obtain quantitative biochemical rates in vivo requires the integration of three major components: compounds labeled with radioisotopes, the positron tomograph, and tracer kinetic mathematical models. These have each been reviewed (*2, 3*) but are briefly discussed below.

Labeled compounds. One of the attractive aspects of the PET technique is that the compounds of interest can be labeled with radioisotopes of natural elements of the biochemical constituents of the body. For example, natural isotopes of carbon, nitrogen, and oxygen are replaced with the short-lived radioisotopes carbon-11, nitrogen-13, and oxygen-15. Fluorine-18 is used as a substitute for hydrogen. These isotopes all decay by the emission of positrons (antielectrons) that combine with electrons to produce two 511–kiloelectron volt gamma rays, which are emitted 180° apart, which easily penetrate the head, and which then allow external detection. The only radioisotopes of these elements that can be detected outside the body are positron emitters. Because carbon, nitrogen, and oxygen are the constituents of virtually all biomolecules and drugs, in principle, an unlimited number of biologically active substrates can be labeled with these radioisotopes without disrupting their biochemical properties (*3, 4*).

Various chemical and biosynthetic procedures have been used to label more than 200 biological substrates and drugs with these isotopes; these labeled compounds constitute a large potential resource for development of bioassay methods with PET (*4*) (Table 1). This list includes labeled amino acids, carboxylic

Michael E. Phelps is Jennifer Jones Simon Professor and Chief, Division of Nuclear Medicine and Biophysics, Department of Radiological Sciences and John C. Mazziotta is an assistant professor, Department of Neurology and Radiological Sciences, UCLA School of Medicine and the Laboratory of Nuclear Medicine Los Angeles, California 90024.

acids, amides, amines, nitriles, alcohols, sugars, hydantoins, steroids, and their derivatives as well as specific substrates, metabolites, analogs, and drugs. Rapid semiautomated techniques have been and continue to be developed to meet the needs of PET, as required by the short half-lives of these isotopes (2 to 110 minutes). Although we discuss only compounds labeled with ^{11}C, ^{13}N, ^{15}O, and ^{18}F, there are also positron-emitting isotopes of Rb, Fe, Mn, Na, K, P, Br, Kr, I, and others.

Positron tomograph. The tomograph consists of an array of radiation detectors that are placed circumferentially around the head and record the emission of γ-rays from the tissue distribution of positron activity. Data collected in this manner are used to form a tomographic image of the cross-sectional distribution of tissue concentration of radioactivity according to the principles of computed tomography (*1*). This provides a quantitative, noninvasive measurement in humans analogous to the well-known invasive techniques of quantitative autoradiography or external counting of resected tissues samples in animal studies. In the invasive techniques, ^{14}C and ^{3}H are commonly used, whereas in PET ^{11}C, ^{13}N, ^{15}O, and ^{18}F are used. This quantitative tissue assay capability of PET provides the means for implementing tracer kinetic methods used throughout the basic sciences.

Tracer kinetic models. The third major component of PET brings together principles of labeled compounds that trace hemodynamic, transport, and biochemical processes, as well as the tissue radioassay capabilities of the tomograph with mathematical models of reaction sequences to provide a framework for calculation of the rates of processes under study. These models, when applied to labeled compounds (tracers) are called tracer kinetic models. The models represent mathematical descriptions of transport or biochemical reaction sequences. Each segment of the sequence is described as a "compartment," and differential equations describe the movement of the natural substrate or labeled compounds (or both) between these compartments. For example, A $\rightleftarrows$ B $\rightleftarrows$ C represents a reaction sequence where A, B, and C are compartments. Measurement is made of the flux between compartments which in turn is used to determine the rate at which the reaction sequence proceeds. These compartments can be separated by membranes where facilitated, active, or passive diffusion may occur or may represent the separation of chemical reactants and products. The configurations for these compartmental models are obtained from knowledge of hemodynamic, transport, and biochemical systems.

For example, a simple two-compartmental model is used in the measurement of oxygen metabolism with $^{15}O_2$. The first compartment is the plasma and the second is tissue where the oxygen is metabolized to water. The rate of transport from the first compartment to the second is described by a rate equation

Table 1. Partial list of compounds labeled with positron-emitting radionuclides.

Cerebral blood flow
$H_2{}^{15}O$, $C^{15}O_2$*, ^{77}Kr, $CH_3{}^{18}F$, ^{18}F-labeled antipyrine, [^{11}C]alcohols, ^{18}F-labeled ethanol

Cerebral blood volume
^{11}CO, $C^{15}O$, ^{68}Ga-labeled EDTA†

Cerebral tissue *p*H
[^{11}C]DMO, $^{11}CO_2$

Transport and metabolism
Oxygen
$^{15}O_2$
Glucose, glucose analogs, and metabolites
2-deoxy-2-[^{18}F]fluoro-D-glucose, 2-[^{11}C]deoxy-D-glucose, [^{11}C]D-glucose, 3-*O*-[^{11}C]methyl-D-glucose, [^{11}C]lactate, -pyruvate, -acetate, -succinate, -oxaloacetate
Amino acids: ^{13}N-labeled
L-[^{13}N]glutamate, -α and ω-glutamine, -alanine, -aspartate, -leucine, -valine, -isoleucine, -methionine
Amino acids: ^{11}C-labeled
L-[^{11}C]aspartate, -glutamate, -valine; D,L-[^{11}C]alanine, -leucine, -tryptophan, -1-aminocyclopentane carboxylic acid, -1-aminocyclobutane carboxylic acid
Free Fatty Acids
[^{11}C]palmitic acid, -oleic acid, -heptadecanoic acid, -β-methylheptadecanoic acid

Molecular diffusion
^{68}Ga-labeled EDTA, ^{82}Rb

Protein synthesis
L-[1-^{11}C]leucine, -methionine, -phenylalanine, L[^{11}C-*methyl*]methionine

Receptor systems
Dopaminergic
[^{18}F]spiperone, [^{11}C]spiperone, [^{75}Br] and [^{76}Br]-*p*-bromospiperone, [^{18}F]haloperidol, [^{11}C]pimozide, [^{11}C]methylspiperone, L-[^{11}C]dopa, [6-^{18}F]-fluoro-L-dopa
Cholinergic
[^{11}C]imipramine, [^{11}C]QNB†
Benzodiazepine
[^{11}C]flunitrazepam, [^{11}C]diazepam, [^{18}F]fluoro valium
Opiate
[^{11}C]etorphine, *N*-methyl-[^{11}C]morphine, -heroin, -carfentanil
Adrenergic
[^{11}C]norepinephrine, [^{11}C]propanolol

Anticonvulsants
[^{11}C]valproate, [^{11}C]diphenylhydantoin

*Converted to $H_2{}^{15}O$ in lungs after inhalation. †QNB, quinuclidinyl benzilate.

from which the rate of tissue extraction and metabolism of oxygen can be determined. As a reaction sequence becomes more complex, the number of compartments will increase. Some principles and aspects of tracer kinetic methods and their use in PET are as follows.

1) The tracer (that is, the labeled compound) is very low in mass compared to the compound being traced, such that there are no significant mass effects that would produce physiologic perturbations altering the system under study. The low mass of these tracers allows PET measurements of reaction rates of substrates with concentrations of less than a few picomoles per gram. However, one can also increase the mass of the tracer compound to make measurements under physiologic loads (for example, drug effects).

2) When the rate of the reaction being studied is not changing during the measurement (steady state), the net reaction rate of any one step in a nonbranching sequence is equal to the net rate of the whole reaction sequence. Thus, measurement of the net initial rates of a reaction sequence with a labeled substrate can be used to assess the net flux of the entire pathway. Alternatively, substrate analogs that isolate one or a small number of steps in a complex reaction sequence can be used to measure the net reaction rate of the whole sequence. Since the analog may have somewhat different reaction kinetics from that of the natural substrate, correction terms based on the principles of competitive reactant or substrate kinetics are used to transform the measured rate of the analog into the corresponding value of the natural compound. These are fundamental principles of the fields of biochemistry and pharmacology. The deoxyglucose model of Sokoloff *et al.* (*5*) is an example of this approach, and under the assumptions of the model has been shown to provide accurate estimates of cerebral glucose utilization rates. Except for Fig. 6b all data on rates of glucose utilization in this article were obtained with the use of 2-deoxy-2-[^{18}F]fluoro-D-glucose (FDG), which, like 2-deoxy-D-glucose (DG) (*5*), has been shown to be an excellent substrate for hexokinase, and like DG, does not undergo further reactions in the glycolytic pathway during the time course of the PET measurements (*6–8*).

3) Although measurements of chemical substrate concentrations are provided by kinetic tracer methods, their use for determinations of chemical reaction rates is more important. Rates of a reaction can change without changes in sub-

strate concentration in the open system of the brain (and the whole body). Changes in tissue substrate concentration are also not specific to the magnitude or direction of changes in rates of reactions.

4) While the chemical form to which the label is attached is known at the time it is intravenously injected or inhaled, the positron tomograph only measures the kinetic changes (changes in time) of tissue concentrations of the label spatially throughout the brain. In order to convert these images of tissue radioactivity concentration to measurements of local reaction rates in vivo, PET measurements must be combined with the time course of the unlabeled or labeled substrate in blood and properly formulated and validated tracer kinetic models. (For example, in determinations of blood flow and volume and of drug interactions only the tracer concentration is required.) With measurements carried out in this manner, the tomograph can provide accurate data on local reaction rates in man.

5) Because of the short half-lives of positron-emitting isotopes it is possible to perform multiple studies in a single setting to observe changes in spontaneous or stimulus-induced alterations in behavior or, using different tracers, for measuring different biochemical processes. For example, ^{15}O measurements can be made in times on the order of 30 seconds and repeated at about 8-minute intervals.

Quantitative PET Methods: Present Status

In autoradiographic studies with ^{14}C-labeled DG, the experiment is terminated 40 minutes after injection of DG. However, in PET with FDG, scans are started and completed within time frames ranging typically from 40 to 100 minutes after injection. Measurements over this time are needed because of (i) the time required to collect enough counts to form the tomographic images of the whole brain, (ii) delays or changes in the study due to problems associated with patients, or (iii) varying time requirements of different types of study protocols (*2, 3*). Because of the longer times between injection and measurement, slow dephosphorylation of FDG 6-phosphate, which is not a usual problem in autoradiography, has been shown to occur and has been taken into account by extending Sokoloff's original model (*5*) to include this reaction (*7*). This restores the accuracy of the model calculation of glucose utilization rates with FDG at these later times and also provides a method for investigating this reaction pathway (*7, 9*).

The lumped constant (LC) in the deoxyglucose model is a term based on the principles of competitive substrate kinetics and accounts for the differences between glucose and deoxyglucose affinities for the transport carrier system and hexokinase. The value of LC has been shown to be regionally invariant in the brain but of a different magnitude in different species; thus appropriate values for the species under study must be used (*5*). Although LC has been shown to be stable during various states such as changes in blood flow and anesthesia induced hypometabolism (*5*), and in chronic human ischemia (*9*), it predictably changes when the rate limiting step shifts from phosphorylation to transport such as in severe hypoglycemia (*10*) and status epilepticus (*10a*). In these cases LC will increase, and the resultant calculated values of glucose utilization will be subject to considerable error if this effect is not taken into account. Anatomical localization and identification of changes in glucose utilization are still correct, but increases and decreases will be overestimated. Methods are being developed for measuring local values of LC to determine when such conditions are encountered and the magnitude of the effect (*11*). The DG and FDG method have also shown excellent agreement with the "gold standard" for measurement of glucose utilization, the Kety/Schmidt method (*12*) that includes measurement of the product of blood flow and the arteriovenous difference for glucose across the brain (*3, 7, 8, 13*).

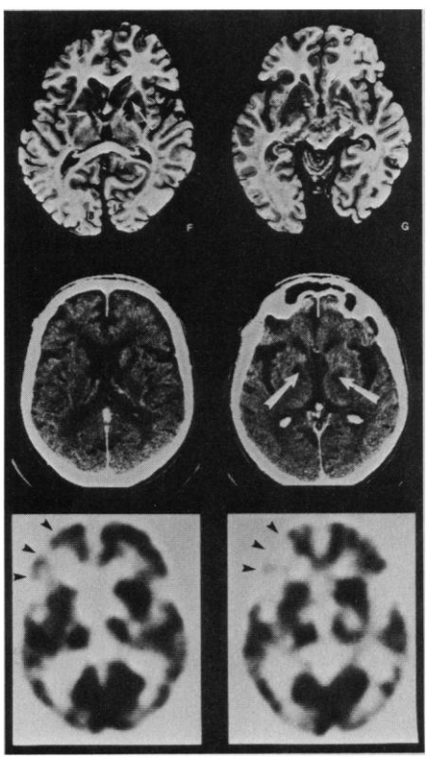

Fig. 1. Structural compared to functional anatomy. Images obtained with three different methods from a patient with multiple infarct dementia. Patient had x-ray CT (center row) and PET studies of glucose utilization with FDG (bottom row) on the same day. Seven days later, the patient died of nonneurological causes; gross and microscopic evaluations of the brain (top row) were then made. The two forms of structural imaging (x-ray CT and postmortem) and the metabolic study with PET both demonstrated multiple small infarctions (arrows) of deep structures of the brain (striatum, putamen, thalamus, and internal capsule). Neither structural imaging techniques demonstrated abnormalities of the cortex. PET, however, demonstrated widespread abnormalities of frontal cortex (glucose utilization decreased 21 percent relative to contralateral side) particularly on the left (arrowheads). These distant effects probably represent disruption of afferent and efferent fiber systems between the frontal cortical areas and subcortical zones, most likely resulting from small subcortical infarcts seen structurally and metabolically. The global rate of glucose utilization was 0.19 μmol min^{-1} g^{-1}, about 30 percent lower than normal age-matched controls. [Courtesy of E. J. Metter, with J. C. Mazziotta and M. E. Phelps, UCLA School of Medicine]

Models based on the principles of tracer kinetics have also been developed for autoradiography and PET with the use of ^{14}C-labeled (*14*) and ^{11}C-labeled (*15*) D-glucose. Although these models are based on the use of natural labeled substrate and therefore have the advantage, compared to DG, that LC=1, by necessity they also contain approximations and correction terms. The most difficult of these is the release of labeled products of metabolism (such as CO_2 and lactate) from the tissue, an effect that must be taken into account by correction terms in the model. To minimize these problems, measurements must be made at early times after injection where errors are larger because of a greater dependence of model parameters on blood flow, blood volume, and the exact values of the rate constants for transport and metabolism of glucose. The retention of the metabolic product (DG-6-phosphate) with DG is advantageous in this respect since it is retained in tissue with a very slow clearance rate. The problems with labeled natural glucose are less difficult with PET because kinetic studies can be performed to measure the variables in the model directly (rather than to use assumed average values) in each experiment. Further studies, nevertheless, are necessary to better understand the magnitude of these issues, and to formulate better models and protocols, and to investigate the value of using glucose la-

beled at selected positions (such as, selective labeling at the carbon -1, -2, -4, or -6 positions).

Quantitative PET methods for oxygen transport and metabolism, blood flow, blood volume, glucose transport, and utilization have been widely used in PET programs around the world (*2*, *3*). Intensive efforts are being focused on the study of tracer kinetic models for determining rates of protein synthesis, amino acid metabolism, tissue *p*H, molecular diffusion through the altered blood brain barrier, and neurotransmitter or receptor interactions with labeled substrates and ligands (Table 1). The results of these projects should provide the basis for some of the PET methods of the future (*3*).

The measurement of biochemical reaction rates with PET requires (i) adherence to the criteria used to develop and structure the tracer kinetic models, and (ii) continuing investigative efforts to better define the accuracy of these methods in all the states of cerebral function and dysfunction to which they will be applied. These requirements are necessary if measurements by different groups of investigators are to be compared. In this regard, PET is no different from any other biochemical measurement where the principles of enzyme and chemical reaction kinetics must be strictly followed.

There are limitations intrinsic to tracer kinetic model approaches along with uncertainties in spatial, temporal, and statistical factors from the tomograph, and we must recognize that ambiguities can arise from the present limited understanding of the biochemical nature of the brain. However, the ability to make such measurements in the living human brain more than compensates for the extensive developmental work which is required in the validation of a new PET method.

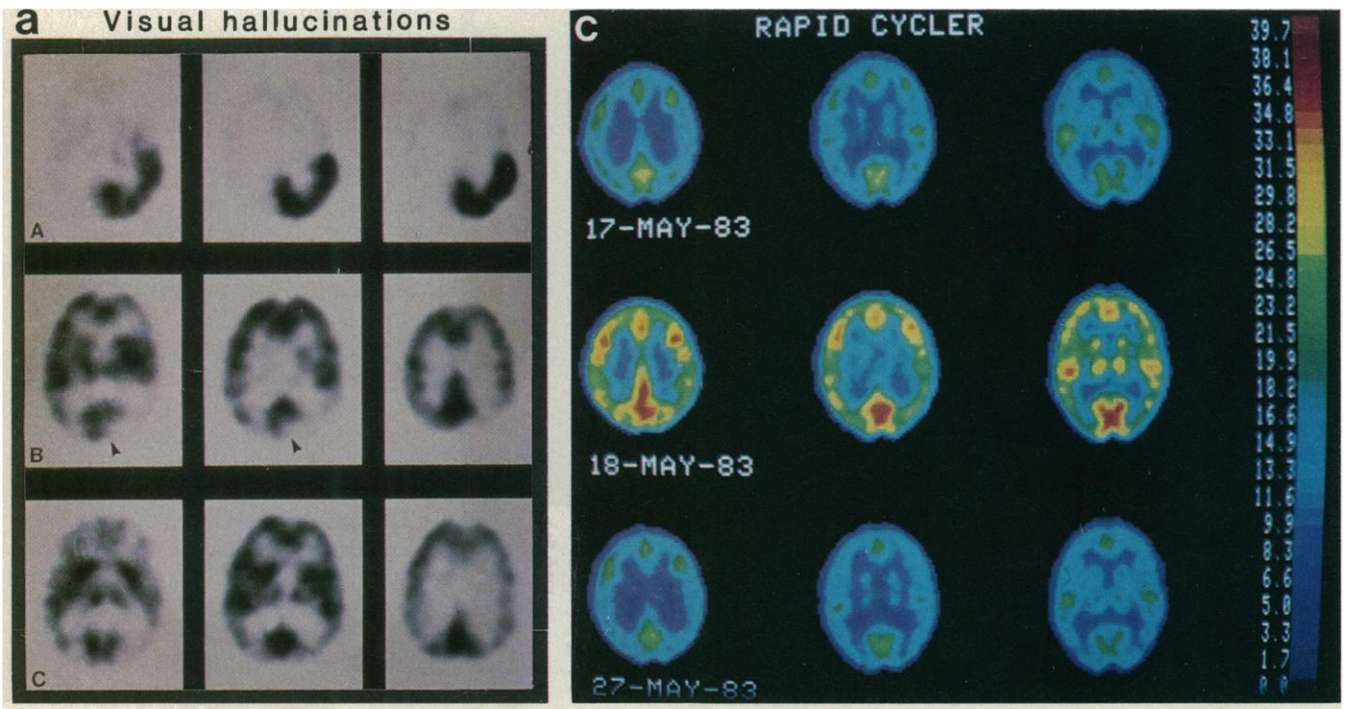

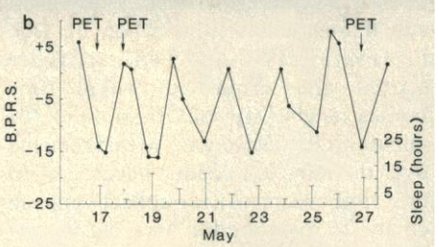

Fig. 2. Pathophysiology of changing behavioral states shown with PET. (a) Patient with complex partial epilepsy studied during seizures (ictal), after seizures (postictal), and after successful therapy (normal). In the ictal state (A) seizures began clinically with formed visual images in left superior quadrant of visual field followed by loss of consciousness and automatisms. Ictal EEG demonstrated discharges in right occipital lobe that quickly spread to the ipsilateral temporal lobe. PET demonstrated increased (284 percent relative to interictal state) glucose utilization in the right occipital and posterior temporal lobes with profound decreases in remainder of brain (42 percent relative to the interictal state). One month after a series of seizures, the patient, in a repeat study showed low glucose utilization (B) in the right occipital and posterior temporal lobes (one third of ictal values) where, during seizure, it was high. The low glucose utilization in the visual cortex (arrows) during this time is consistent with the patient's loss of vision in left visual field (homonymous hemianopia). After drug therapy, the patient remained seizure-free for 1 year. The glucose utilization during this time returned to normal (C), consistent with the resolution of the left visual field deficit. These studies show that PET can be used to detect both positive (hallucinations) and negative (visual field deficit) clinical manifestations of an epileptic disorder and the reversal of these changes resulting from treatment and clinical resolution of symptoms. The x-ray CT study was normal and unchanged in each state. [From Engel *et al.* (*18*); courtesy of *Neurology*] (b) Graph of the mood fluctuations of a rapid cycling bipolar (manic-depressive) affective disorder patient. The patient cycled between mood states every 24 to 48 hours. The modified brief psychiatric rating scale on the left (B.P.R.S.) indicates relative mania (positive values) and relative depression (negative values). Sleep cycles varied in parallel with mood swings. Three studies of cerebral glucose utilization with PET were obtained, two during depressive states and one during hypomania. [From Baxter *et al.*, in (*22*); courtesy of *Archives of General Psychiatry*] (c) Glucose utilization images of the rapid cycling bipolar patient described in (b). The scale to the right is glucose utilization rates in micromole per minute per 100 grams. Studies on 17 May 1983 and 27 May 1983 were made when the patient was in depressed state; the study on 18 May 1983 was made during a hypomanic state. Global reductions in glucose utilization (relative to the scan obtained during hypomania) can be seen for the two studies obtained in the depressed state. The global supratentorial increase in glucose utilization from depression to hypomania was about 40 percent. The global glucose utilization rate in the hypomanic state is not significantly different from that of age-matched normals. These studies demonstrate the ability of PET to provide pathophysiological insights into abnormal behavior that occurs as either a manifestation of epilepsy or psychiatric disorders. [From Baxter *et al.*, in (*22*); courtesy of *Archives of General Psychiatry*]

Applications of PET

Cerebral organization and structure-function relationships. Methods used to investigate the structural nature of the human brain include in vivo techniques, such as x-ray computed tomography (CT) and proton nuclear magnetic resonance (NMR) CT, and postmortem techniques. Relatively little information exists about local biochemical and physiological processes of the human brain in vivo. Knowledge of the functional organization of the human brain has, however, been obtained through PET studies of both normal individuals and patients with cerebral disorders. Such studies provide a more comprehensive view of cerebral organization than structural studies alone (Fig. 1), particularly when one attempts to correlate the resulting data with behavioral observations of the subject.

Since all diseases of the brain result from or produce biochemical alterations, functional images that display such processes have demonstrated earlier, larger, and more distributed lesions than those found in anatomically oriented techniques including detailed postmortem evaluations (Fig. 1). Examples of the mismatch between structural and functional lesions have been demonstrated in patients with seizure disorders (Fig. 2a), dementing processes (Fig. 3), neurodegenerative diseases (Fig. 3), and acute cerebral infarcts (see Fig. 5).

Since the brain consists of large numbers of interconnected substructures, damage to one structure or its interconnecting fiber bundles will also result in functional effects at multiple sites throughout any given network. PET has revealed this distributed organization, leading to a more comprehensive view of human functional brain systems in health and disease. Traditional clinical-pathological correlations that have been the mainstay of symptom-lesion localization in the brain may soon give way to "clinical-physiological correlations" (*16*) that can be performed in vivo with PET.

Structural evidence has been scant in the search for the basis of a number of human cerebral disorders. Examples of entities in this category would include psychiatric syndromes, many forms of

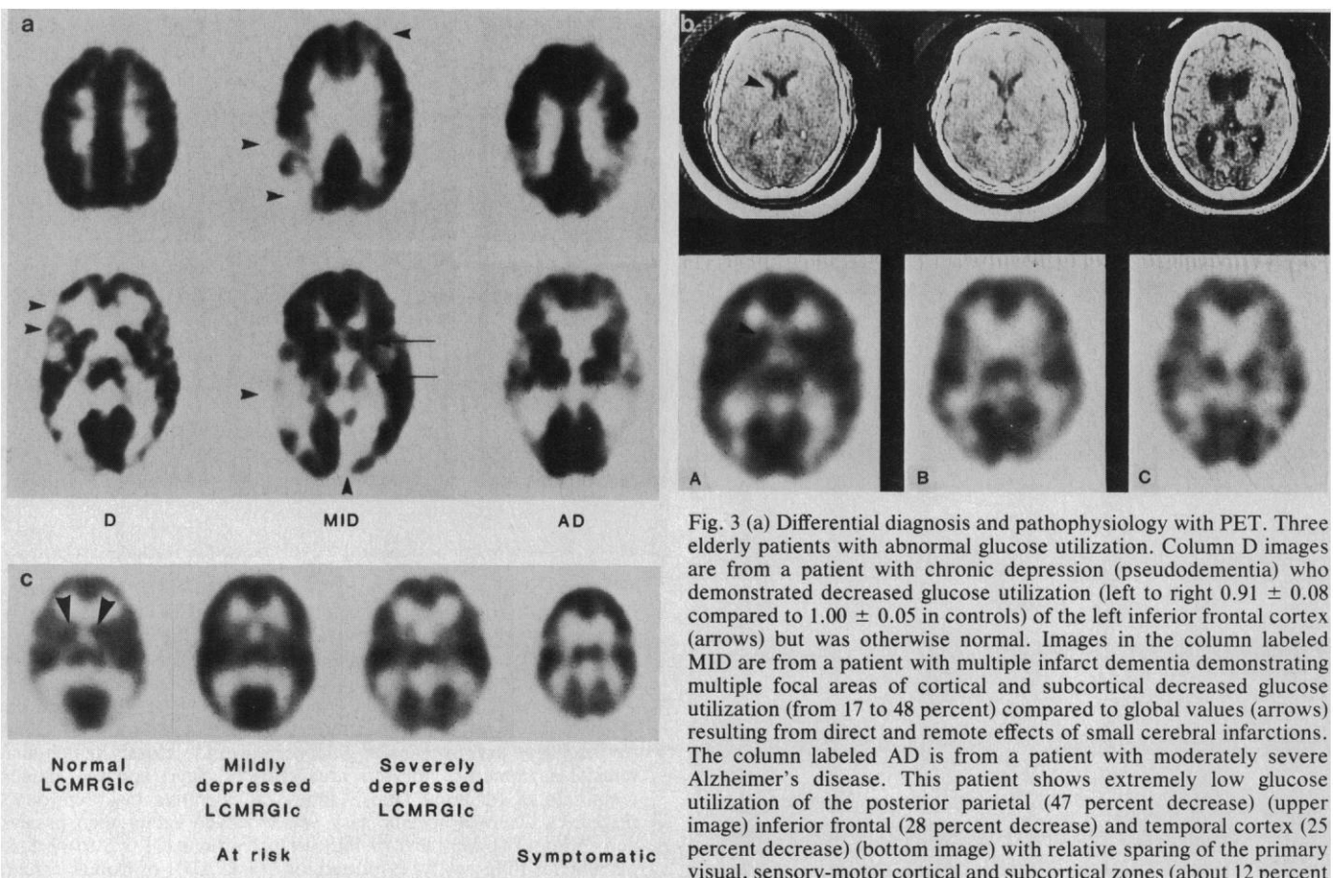

Fig. 3 (a) Differential diagnosis and pathophysiology with PET. Three elderly patients with abnormal glucose utilization. Column D images are from a patient with chronic depression (pseudodementia) who demonstrated decreased glucose utilization (left to right 0.91 ± 0.08 compared to 1.00 ± 0.05 in controls) of the left inferior frontal cortex (arrows) but was otherwise normal. Images in the column labeled MID are from a patient with multiple infarct dementia demonstrating multiple focal areas of cortical and subcortical decreased glucose utilization (from 17 to 48 percent) compared to global values (arrows) resulting from direct and remote effects of small cerebral infarctions. The column labeled AD is from a patient with moderately severe Alzheimer's disease. This patient shows extremely low glucose utilization of the posterior parietal (47 percent decrease) (upper image) inferior frontal (28 percent decrease) and temporal cortex (25 percent decrease) (bottom image) with relative sparing of the primary visual, sensory-motor cortical and subcortical zones (about 12 percent decrease). Alzheimer's disease patients have also shown an average decrease of global supratentorial glucose utilization (33 percent), compared to age-matched normal control subjects, with the major abnormalities occurring in neocortical zones. This study demonstrates the differential diagnostic capability of PET to separate patients with processes affecting mental abilities based on pathophysiological patterns observed in the functional images. Stated values are for groups of patients. Errors are standard deviations. [From D. E. Kuhl *et al.* (*47*); courtesy of *Radiology*] (b) Functional abnormalities in Huntington's disease: x-ray CT (top row) and local cerebral glucose utilization with PET (bottom row) in Huntington's disease. Left column is from a normal subject and demonstrates the normal structure and glucose utilization of the caudate nucleus (arrows). Patient in center column has early clinical symptoms of Huntington's disease and demonstrates a normal structural appearance of the caudate nucleus on x-ray CT image but decreased glucose utilization in caudate and adjacent basal ganglia structures (putamen and globus pallidus). The column at the right is a patient with late Huntington's disease and demonstrates both structural (cortical and subcortical atrophy) and functional abnormalities of the caudate and putamen bilaterally. [From D. E. Kuhl *et al.* (*31*); courtesy of *Annals of Neurology*] (c) Subjects at-risk for Huntington's disease. Image at far right is from a patient with symptomatic Huntington's disease demonstrating loss of glucose utilization of the basal ganglia as was seen in (b). The three images on the left are all from asymptomatic at-risk subjects (offspring of Huntington's disease patients) each having a 50 percent chance of developing the disorder. In this group (15 subjects) about half of the patients have demonstrated a normal glucose utilization pattern while the other half show mild to severely depressed glucose utilization in the caudate. The at-risk subjects were symptom free at the time of the study. This study indicates that PET may serve to identify physiological abnormalities that not only precede structural changes in the brain but also preceded the onset of symptoms in susceptible subjects. [From D. E. Kuhl *et al.* (*31*); courtesy of *Annals of Neurology*]

epilepsy, and various developmental disorders of the brain. In patients with partial seizure disorders (symptoms referable to a limited region of the brain), interictal studies (between seizures) with FDG have identified areas of decreased glucose utilization in 70 percent of affected individuals (Fig. 2a) (*17*). These zones could be correlated with the site of maximal abnormalities determined by surface and depth electrode electrophysiological techniques, and were found to be extremely specific in identifying sites of microscopic pathology not detected by the conventional radiological imaging techniques such as x-ray CT, angiography, and pneumo-encephalography (*17*). During seizure activity (ictal period), sites that show low glucose utilization interictally show increased utilization (often increasing by 100 to 200 percent) (Fig. 2a); this suggests that the interictal low glucose utilization is at least in part due to nonstructural causes (*17, 18*). The sites of increased glucose utilization during the ictal phases of partial seizures correlated both with the behavior of the patient and with spikes recorded from scalp and particularly depth electroencephalographic (EEG) recordings (Fig. 2a) (*17, 18*). Patients with generalized forms of epilepsy (such as major motor or petit mal seizures) have global (that is, throughout the brain) increases in glucose utilization in the ictal period of seizure activity with subsequent depression in glucose utilization in the postictal period (*19*).

The finding of interictal zones of hypometabolism, particularly in the temporal lobe of partial epilepsy patients, has suggested that this may be specific for a lowered threshold or greater susceptibility of these foci to initiation of seizure activity. These findings have in turn promoted a series of parallel studies in animals (glucose utilization, blood flow, morphology, electrophysiology, ligand

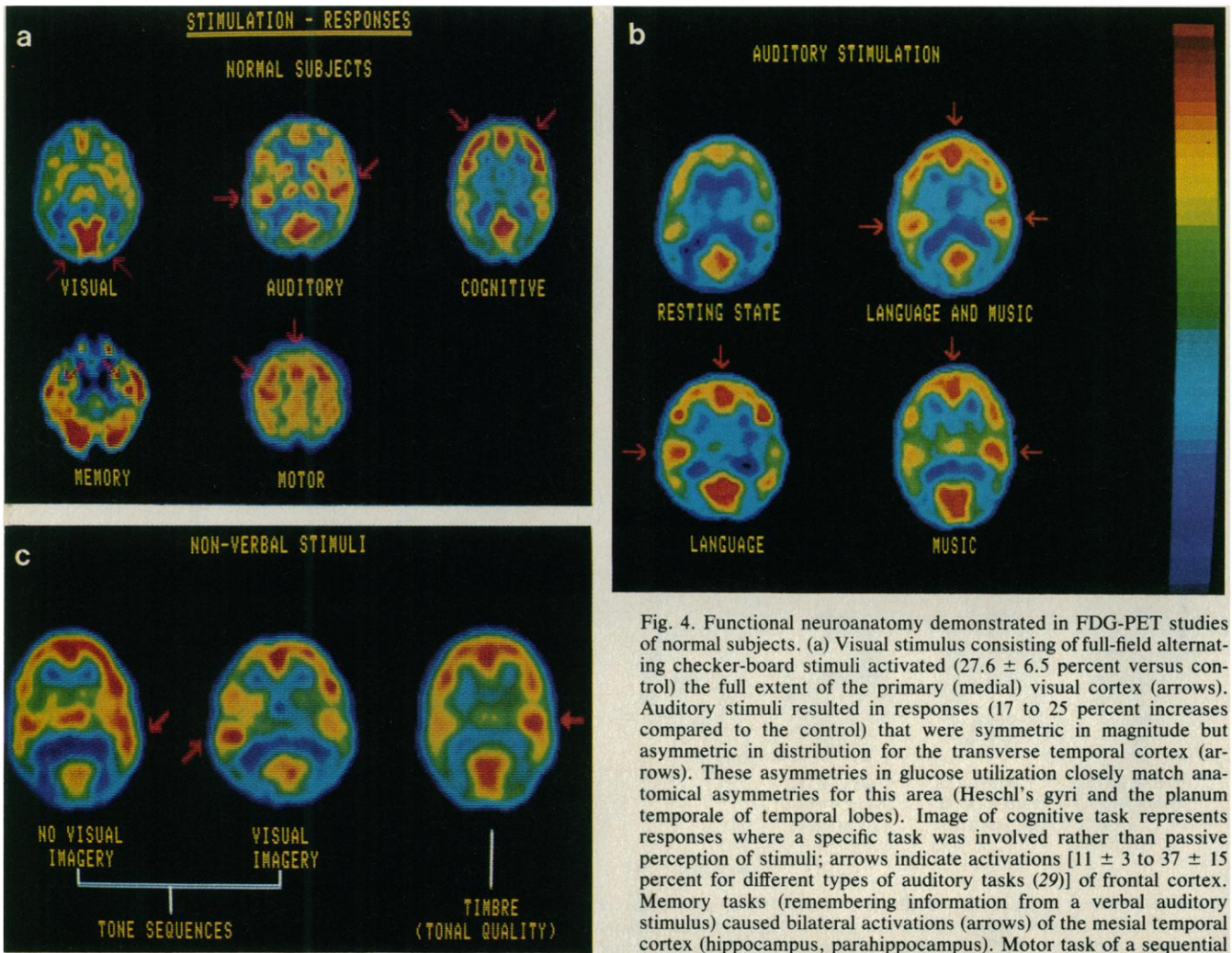

Fig. 4. Functional neuroanatomy demonstrated in FDG-PET studies of normal subjects. (a) Visual stimulus consisting of full-field alternating checker-board stimuli activated (27.6 ± 6.5 percent versus control) the full extent of the primary (medial) visual cortex (arrows). Auditory stimuli resulted in responses (17 to 25 percent increases compared to the control) that were symmetric in magnitude but asymmetric in distribution for the transverse temporal cortex (arrows). These asymmetries in glucose utilization closely match anatomical asymmetries for this area (Heschl's gyri and the planum temporale of temporal lobes). Image of cognitive task represents responses where a specific task was involved rather than passive perception of stimuli; arrows indicate activations [11 ± 3 to 37 ± 15 percent for different types of auditory tasks (*29*)] of frontal cortex. Memory tasks (remembering information from a verbal auditory stimulus) caused bilateral activations (arrows) of the mesial temporal cortex (hippocampus, parahippocampus). Motor task of a sequential finger movement of the right hand caused cortical metabolic activation (18.6 ± 3.9 compared to the control) of the left motor strip (lower arrow) and supplementary motor cortex (vertical arrow). Errors are standard deviations. [Courtesy of M. E. Phelps and J. C. Mazziotta, UCLA School of Medicine] (b) Auditory stimuli produced metabolic responses that varied with the content and in some cases strategy used by the subject to perform the task. In resting states (ears plugged, eyes open) left-right cerebral symmetry (left/right = 1.01 ± 0.03) in glucose utilization is seen. Verbal auditory stimuli predominantly activated and caused metabolic asymmetries (left > right = 5 to 16 percent) of the left hemisphere while nonverbal stimuli (music) predominantly activated the right hemisphere (16 to 27 percent) in right-handed individuals. Simultaneous stimulation with language and music caused bilateral activations of both hemispheres. [From J. C. Mazziotta *et al.* (*29*); courtesy of *Neurology*] (c) Nonverbal auditory stimuli caused activations of the language nondominant (right) hemisphere. The timbre test required subjects to compare complex chords for similarities and differences and consistently produced increases (22 percent versus control) in glucose utilization in the right hemisphere (image at right, arrow). This test did not contain any temporal sequences of notes that can be analytically perceived. The chord pairs differed only in tonal quality. When subjects were asked to identify differences and similarities in sequences of notes (tone sequences) the side of maximal activation correlated with the strategy used by the subject to perform the task. Color scale is in units of micromoles per minute per 100 g, ranging from 2 (dark purple) to 45 (red). See text for description. [Modified from J. C. Mazziotta *et al.* (*29*); courtesy of *Neurology*]

assays) (*20*) and in humans (glucose utilization, oxygen metabolism, and blood flow) with PET in ictal, postictal, and interictal states (*17–19, 21*) along with morphological and ligand studies in surgically resected tissue samples. This illustrates the manner in which PET, animal, and laboratory assays can be assembled to study the underlying mechanisms of a human disorder.

In drug-free patients with bipolar (manic-depressive) mood disorders, measurements with FDG and PET have shown changes throughout the brain in glucose utilization during different mood states (Fig. 2, b and c). During the depressive phase of illness, patients demonstrated reductions in glucose utilization of about 25 percent throughout the supratenorial structures of the brain which were significantly ($P < 0.001$) below those of age- and sex-matched normals (*22*).

The same patients, when later studied in hypomanic (state between normal and mania) phases of the illness, showed glucose utilization rates that were not significantly different from those of age- and sex-matched controls. Although the major changes in glucose utilization seen thus far have been global, the largest differences between behavioral states occurred in the frontal and anterior cingulate cortices (*22*). Patients with unipolar mood disorders (depression) in drug-free states were found to have global supratentorial cerebral glucose utilization values that were not significantly different from age- and sex-matched controls. However, these patients did exhibit significantly depressed glucose utilization (15 percent lower than age- and sex-matched normals) bilaterally in the striatum (*22*). This reduced striatal glucose utilization recovered to normal levels in patients who became euthymic (that is, normal mood) spontaneously or by drug therapy (*22*).

Physiological psychology. Many methodologies have been used in the study of normal cerebral function. These approaches have included neuropsychological, electrophysiological, and behavioral observations of human subjects performing various tasks. Studies in animals by means of biochemical, electrophysiological, and autoradiographic techniques have also been used to define the anatomical and functional organization of the brain during defined tasks. In a similar manner, PET provides a means of studying local sensory, motor, memory, and cognitive function in normal subjects in vivo (Fig. 4). Thus, much in the way Penfield and his colleagues (*23*) mapped cerebral function through intraoperative stimulation of the human cerebral cortex, PET can provide physiological and biochemical information about normal cerebral function for all human brain regions in a noninvasive fashion.

Various sensory and motor stimulation tasks (Fig. 4) have been used to define the functional neuroanatomy of the human brain. Visual stimulation studies, with ^{15}O-labeled water to measure cerebral blood flow, or with FDG to measure glucose utilization have revealed some of the normal physiological response characteristics of the human visual cortex (*24–28*). These studies have shown (i) the topography of the human visual cortex relative to the site and size of retinal stimulation (*24*), (ii) that the magnitude of blood flow or glucose utilization of the visual cortex is a function of stimulus complexity (*25, 26*) and rate (*16*), (iii) that functionally 50 percent of the input from each eye goes to each visual cortex (*25, 26*), and (iv) that lesions of the visual system (both within and outside the visual cortex) produce

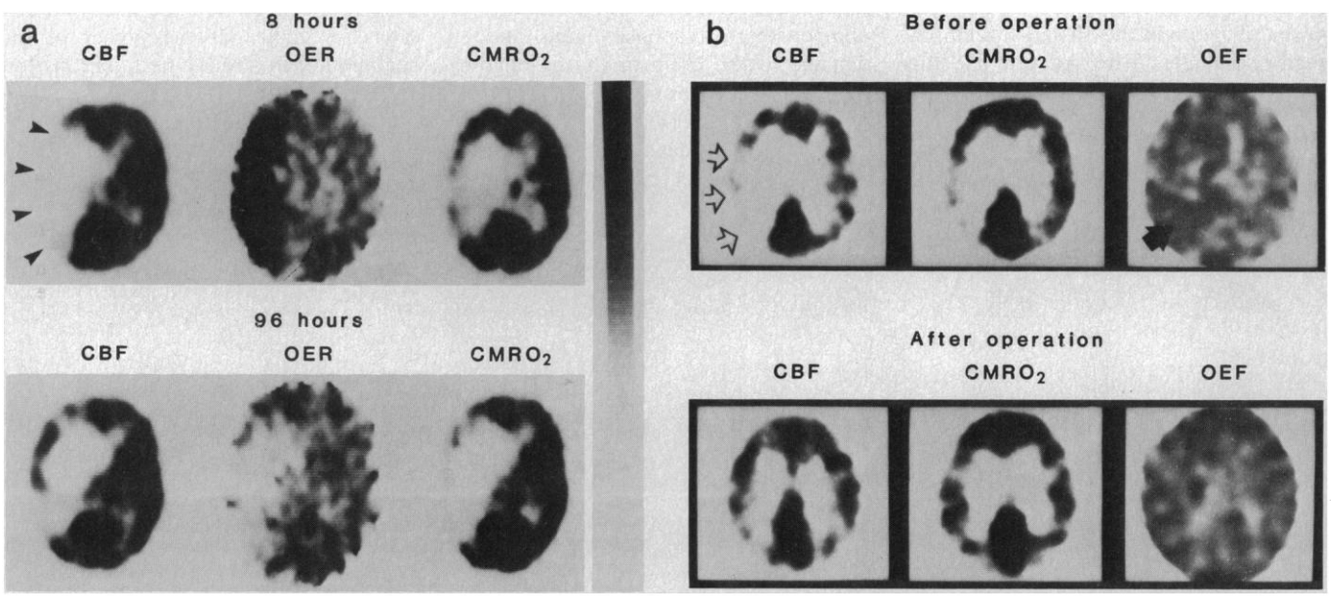

Fig. 5. Pathophysiology of cerebrovascular disease. (a) A patient with left hemisphere cerebral ischemia studied 8 and 96 hours after the onset of symptoms. During both intervals cerebral blood flow (CBF), oxygen extraction ratio (OER), and oxygen metabolism ($CMRO_2$) were determined. The blood flow 8 hours after the stroke was severely depressed in the left middle cerebral artery distribution. Oxygen utilization was also reduced although not as severely as blood flow. The resultant mismatch accounts for increased oxygen extraction [mean value at 14 hours after symptom onset = 0.71 ± 0.12 (R. J. Wise *et al.*, in *34*), normals = 0.49 ± 0.02 (R. S. Frackowiak *et al.*, in *34*) in the viable but jeopardized zone. At 96 hours, blood flow became heterogenous in the area probably because of failure of vascular autoregulatory mechanisms and oxygen utilization has fallen further. Oxygen extraction is now sharply reduced below normal, indicating irreversible brain injury and predicting infarction for this zone. Errors are standard deviations. [From R. S. Frackowiak and R. J. Wise, in (*34*); courtesy of *Neurology Clinics*] (b) Patient with left internal carotid artery occlusion before and after superficial temporal artery-middle cerebral artery bypass surgery. Preoperatively, patient had symptoms referable to the left hemisphere including clumsiness of the right hand and difficulties with language. Blood flow studies with PET demonstrated moderately severe reductions of flow in the cortex of the left parietal lobe with mild reductions in oxygen utilization. The mismatch between flow and metabolism resulted in an increased oxygen extraction fraction (OEF) (arrow in OEF image), an indication that the tissue is viable although in a precarious state. After bypass surgery the patient's symptoms resolved and the blood flow, oxygen extraction, and oxygen metabolism all returned to normal. Both pre- and postoperatively the x-ray CT images of the patient were normal. [From J. C. Baron *et al.* (*36*); courtesy of *Stroke*]

functional abnormalities that can be correlated with the patients' clinical syndromes despite a lack of anatomical alterations detectable by x-ray CT (*26, 28*) (Fig. 2a).

Studies of the human auditory system with FDG indicate a correlation between the distribution of glucose utilization and the content of the stimulus (Fig. 4b) and, in some cases, the strategy used by the subject to solve the task (Fig. 4c) (*29, 30*). While complex patterns of these responses to auditory stimuli were observed, verbal stimuli caused asymmetric increases in glucose utilization in the left hemisphere in right-handed individuals (Fig. 4b). Nonverbal stimuli, such as musical chords, activated primarily right hemisphere areas particularly in the inferior frontal, parietal, and superior temporal regions (Fig. 4b) (*29, 30*). In subjects who listened to sequences of musical notes (*29*) and were asked to determine whether notes in one sequence differed from those in another, the pattern of glucose utilization correlated with the strategy used by the subject (Fig. 4c). Individuals who used specific visual imagery and analytical strategies ("visualizing" frequency histograms or musical scales in their minds for comparing note sequences) had predominantly left hemisphere asymmetries and increases in glucose utilization in the posterior temporal region. Subjects who did not use this strategy to solve the task but rather used mental "resigning" of the notes had activations in the inferior parietal and temporal-occipital regions of the right hemisphere (Fig. 4c) (*29*).

In general, in studies of subjects with PET, when a specific task was involved rather than the mere passive perception of stimuli, frontal cortical zones showed greater glucose utilization (*29, 30*) (Fig. 4a). In addition, subjects who were asked to recall specific aspects of auditory stimuli had activations of the mesial temporal lobe (hippocampus, parahippocampus) that were never seen in situations where auditory perception without memory tasks were required of the subject.

While the study of normal cerebral function through PET is interesting in itself, the above-mentioned tasks can also be useful in seeking a better understanding and improved differential diagnosis of cerebral disorders (*30*). Thus, much in the way a cardiologist imposes physical exercise on patients to induce detectible changes in altered myocardial function, so too the neuroscientist can induce cerebral work by the use of neurobehavioral or pharmacological cerebral stimuli. This approach may reveal subtle or early cerebral dysfunction that is at or near the limit of functional reserve of the brain.

Stimulation tasks can also be used to investigate cerebral reorganization or compensatory responses after sudden damage to the brain or during ongoing structural degeneration of the brain in certain disorders (*30*). The resulting data should provide clues as to how the brain functionally reorganizes or adapts to perform a task when the system identified for the normal performance of that task has been compromised by cerebral pathology.

Cerebral stoichiometry and pathophysiology of disease. The normal brain has a fairly constant stoichiometry among various substrate utilization rates, and changes in these relationships should be sensitive in detecting and providing insights in the mechanisms of early derangements of cerebral systems induced by disease. Such changes may also be critical in determining the type and timing of treatment. By examining a large number of biochemical and physiological processes in normal subjects with PET, one can define the normal relation between these processes and their range of variability. Once known, these relations can be examined in disease states. Serial studies in patients with cerebral disorders, with multiple tracers to determine cerebral stoichiometry as a function of time, can help identify the pathophysiological sequence of events that occurs during the expression of a syndrome. Similarly, one can examine the stoichiometrically changing relations that occur as the disease advances, as the patient recovers from the disease, or as a result of therapeutic interventions. Some examples of the power of this technique can already be found in studies performed with PET (*31, 33–39*) (Figs. 5 and 6).

Huntington's disease is an inherited

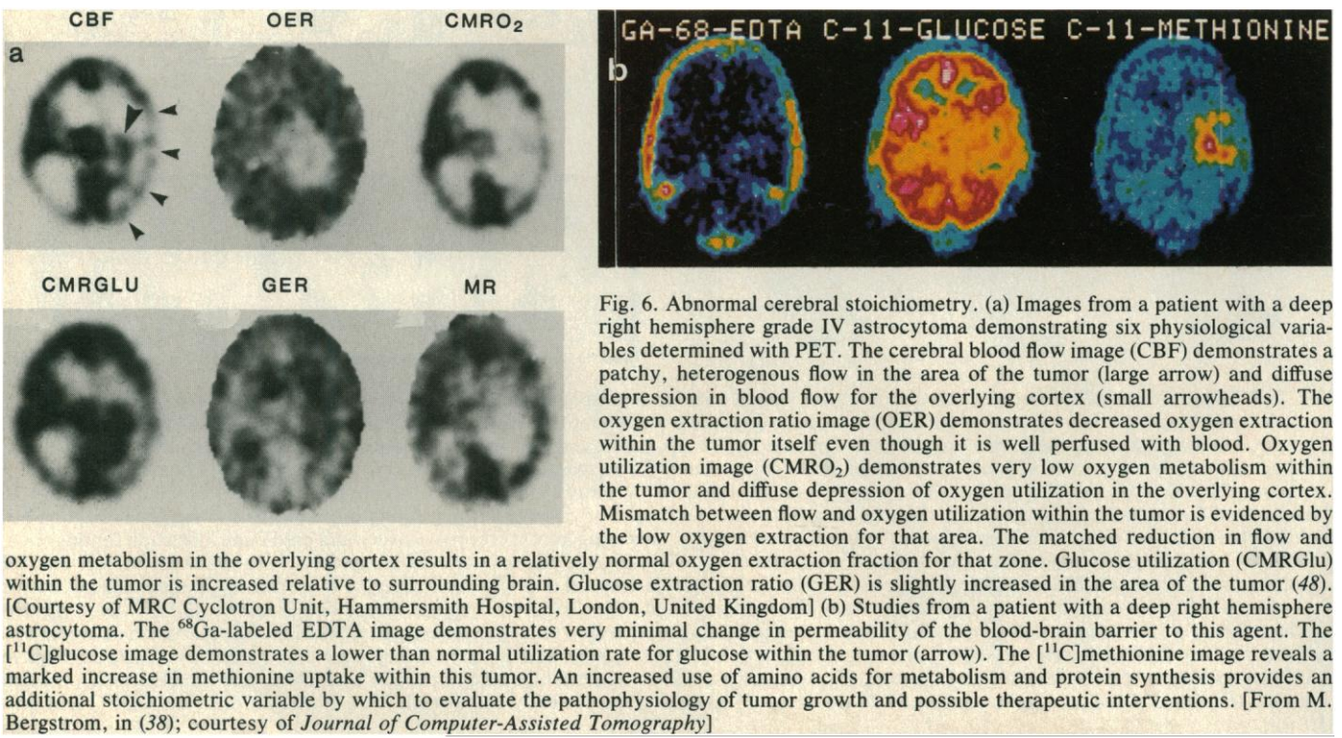

Fig. 6. Abnormal cerebral stoichiometry. (a) Images from a patient with a deep right hemisphere grade IV astrocytoma demonstrating six physiological variables determined with PET. The cerebral blood flow image (CBF) demonstrates a patchy, heterogenous flow in the area of the tumor (large arrow) and diffuse depression in blood flow for the overlying cortex (small arrowheads). The oxygen extraction ratio image (OER) demonstrates decreased oxygen extraction within the tumor itself even though it is well perfused with blood. Oxygen utilization image ($CMRO_2$) demonstrates very low oxygen metabolism within the tumor and diffuse depression of oxygen utilization in the overlying cortex. Mismatch between flow and oxygen utilization within the tumor is evidenced by the low oxygen extraction for that area. The matched reduction in flow and oxygen metabolism in the overlying cortex results in a relatively normal oxygen extraction fraction for that zone. Glucose utilization (CMRGlu) within the tumor is increased relative to surrounding brain. Glucose extraction ratio (GER) is slightly increased in the area of the tumor (*48*). [Courtesy of MRC Cyclotron Unit, Hammersmith Hospital, London, United Kingdom] (b) Studies from a patient with a deep right hemisphere astrocytoma. The ^{68}Ga-labeled EDTA image demonstrates very minimal change in permeability of the blood-brain barrier to this agent. The [^{11}C]glucose image demonstrates a lower than normal utilization rate for glucose within the tumor (arrow). The [^{11}C]methionine image reveals a marked increase in methionine uptake within this tumor. An increased use of amino acids for metabolism and protein synthesis provides an additional stoichiometric variable by which to evaluate the pathophysiology of tumor growth and possible therapeutic interventions. [From M. Bergstrom, in (*38*); courtesy of *Journal of Computer-Assisted Tomography*]

disorder manifested by dementia, abnormal movements, and psychiatric symptoms. The offspring of affected individuals have a 50 percent chance of inheriting the abnormal gene and manifesting the disease. The clinical manifestations typically do not appear until the third or fourth decade of life. Thus, a population exists that is at risk for the disease. These individuals may have subclinical expression of symptoms although previous attempts to identify such presymptomatic patients have been, until recently, unreliable.

In PET studies with FDG, all patients with Huntington's disease showed a reduction in glucose utilization in the striatum (up to 70 percent reductions), the portion of the brain with the most profound structural changes (neuronal cell loss) in the advanced stages of this disorder (*31*). In those patients who were just beginning to manifest symptoms of this disease, structural imaging techniques such as x-ray CT were normal (Fig. 3b), but investigations with FDG and PET revealed profound reductions in glucose utilization in the striatum (*31*).

In a group of 15 asymptomatic individuals who were at-risk for Huntington's disease, about half demonstrated mild-to-moderate (up to 40 percent) reductions in glucose utilization for the caudate nucleus (Fig. 3c) (*31*). Three of the individuals with these abnormalities subsequently developed symptoms (*31*). Thus, PET can identify functional lesions in Huntington's disease that precede gross structural changes in the brain (as determined by x-ray CT) and appears to be able to identify abnormalities in patients even before symptoms of the disease are manifest (namely, changes that are still within the compensatory mechanisms of the brain). The relation of these presymptomatic changes in glucose utilization with the presence of the abnormal gene (*32*) remains to be determined.

Serial studying of at-risk individuals with various positron labeled tracers from early ages through the onset of symptoms can provide a detailed description of the regional changes in brain biochemistry as a function of time along with a correlation of these changes with clinical symptoms. Since experimental treatments for such disorders would be most successful when used in presymptomatic or early stage subjects, PET may be useful in identifying those subjects and in providing more objective evidence as to whether such therapeutic interventions are beneficial or harmful.

Patients with cerebrovascular disease (Fig. 5) have been studied with PET to understand better the relationship of cerebral blood flow with oxygen metabolism and extraction (*16, 33–37*). These studies have provided some initial insights into the compensatory mechanisms used by the brain to maintain tissue viability despite decreased substrate availability. As blood flow to the brain is decreased (in the initial minutes and hours after the onset of stroke symptoms), the percentage of arterial oxygen extracted into cerebral tissue increases to a maximal level in order to maintain oxidative metabolism (*34*). Subsequently, the capacity of this and other compensatory mechanisms can be exhausted, and if so, oxygen metabolism will fall. This appears to occur at an oxygen utilization rate of about 0.58 micromoles per minute per gram of tissue (*35*). Along with this change, the percentage of oxygen extracted by cerebral tissue also declines, an indicator of irreversible tissue damage (Fig. 5). The measurement of oxygen extraction and utilization has proved to be a much more reliable predictor of tissue degeneration than blood flow alone since the latter can be decreased, normal, or even increased (reactive hyperemia) at different stages or times in the progressive development of cerebral ischemia and infarction (*16, 33, 34*). These measurements have been combined to select patients for therapeutic intervention and to monitor the effectiveness of the treatment (Fig. 5) (*36, 37*).

Patients with brain tumors have been studied with several positron labeled tracers (Fig. 6) in order to (i) assess their pathological stoichiometry (*38, 39*), (ii) identify differences in these relations for different tumor grades (*39*), and (iii) predict and evaluate the effects and response of a given tumor to a specific radio- or chemotherapeutic modality (*40*). The combined knowledge of energy

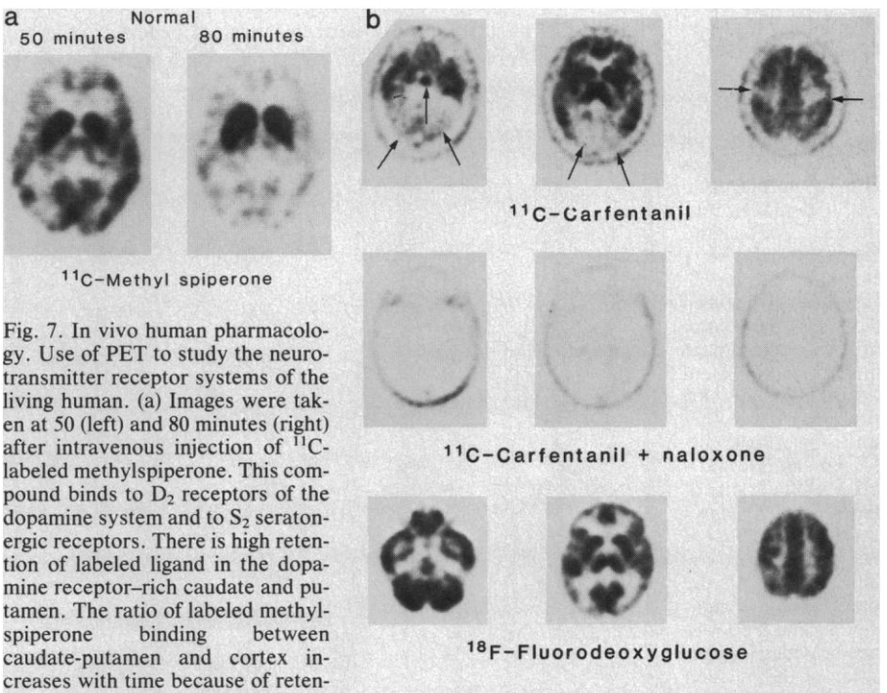

Fig. 7. In vivo human pharmacology. Use of PET to study the neurotransmitter receptor systems of the living human. (a) Images were taken at 50 (left) and 80 minutes (right) after intravenous injection of ^{11}C-labeled methylspiperone. This compound binds to D_2 receptors of the dopamine system and to S_2 seratonergic receptors. There is high retention of labeled ligand in the dopamine receptor–rich caudate and putamen. The ratio of labeled methylspiperone binding between caudate-putamen and cortex increases with time because of retention on the D_2 sites as compared to clearance from nonspecific binding sites and S_2 receptors in the cortex. Ratio of radioactivity in caudate to cerebellum in right-hand image is 4.4. This study also illustrates the high sensitivity of PET to detect concentrations of picomoles per gram or less. [From Wagner *et al.*, in (*42*)] (b) Opiate receptors in human brain. The PET images in the top row were obtained 30 to 60 minutes after intravenous administration of 25 mCi of [^{11}C]carfentanil (80 ng/kg), a mu opiate antagonist. The three images are 7.2 cm, 4 cm, and 0.8 cm above the canthomeatal line (far right to left). Images in the middle row were acquired 30 to 60 minutes after intravenous administration of (1 mg/kg) naloxone (the + isomer), which is an opiate antagonist, and the same dose of [^{11}C]carfentanil used in the first study. In the top row a preferential accumulation of activity is seen in areas rich in opiate receptors such as the thalamus, basal ganglia, and frontal cortex (center and right-hand images) and pituitary gland (left-hand image; inner arrow). Low activity is seen where opiate receptors exist in low concentration, such as the occipital cortex (center image, arrows), the postcentral gyrus (right-hand image; arrows) and the cerebellum (left-hand images; arrows). Images in the middle row demonstrate the low level of nonreceptor binding when labeled carfentanil binding is blocked with naloxone. Approximately 90 percent of specific opiate receptor binding in the thalamus and basal ganglia is displaced. The outer rings in the images result from ^{11}C activity in scalp. Images in the bottom row represent glucose utilization (FDG) for approximately the same levels as the opiate receptor distribution study. [Carfentanil studies from J. J. Frost *et al.*, in (*43*) and glucose utilization images from M. E. Phelps *et al.*, in (*3*)]

metabolism and protein synthesis for assessing cell turnover rates and tumor growth before and after therapy can be evaluated with PET (Fig. 6). For example, radiation therapy is more effective in patients with tumors having high oxygen concentrations (because of the generation of free radicals) than in patients with tumors having low oxygen concentrations (Fig. 6). The determination of the degree of malignancy of cerebral gliomas in vivo with PET measurements of glucose utilization correlates well with histological grading of biopsied or resected samples—that is, an increasing degree of malignancy was associated with increasing rates of glucose utilization as measured with FDG (*39*).

The reliability and appropriateness of animal models of human diseases are frequently questioned. The ability to compare animal models and human conditions through, for example, biochemical assays with the tracer kinetic approach provides the opportunity to scrutinize these animal models and compare differences and similarities with the human disease. Animal models of different aspects of epilepsy, neoplastic diseases, psychiatric disorders, Parkinson's and Huntington's diseases, and others can be examined by quantitative autoradiography and biochemical assays for comparison with PET studies of patients having these disorders. Similarities and differences in stoichiometry, structure-function relationships, behavior-function relationships, and drug responses with PET can help in the choice of appropriate models. The selected animal model can then be studied by histological, biochemical, and electrophysiologic techniques that are either too invasive or too logistically complex to be performed in humans. Hypotheses resulting from studies on mechanisms of the disease in animals can then be tested in humans with PET.

In vivo pharmacology. The neuropharmacology of the human brain can be examined with PET through the use of two different strategies. In the first, pharmacological doses of drugs can be administered to normal subjects and patients with cerebral disorders and their effect on processes such as blood flow and metabolism can be examined to determine the anatomical sites where drug-induced alterations in biochemical processes occur (*41*). Alternatively, the drug itself can be labeled with a positron-emitting isotope (Table 1) and its pharmacokinetic behavior (*42–45*) can be examined directly in vivo under conditions where the drug is present in tracer amounts (that is, with no mass effect) or in concentrations where pharmacological effects are produced (Fig. 7). Either way, biochemical assays can be performed to examine the pharmacological effects of specific agents on behavior, symptoms, and structure-function relationships in the human brain and to identify neurochemical systems involved in specific diseases. The anatomical sites of these effects can be correlated with neurochemical systems associated with such sites in the brain as determined through in vitro studies of human tissue or animal studies of these systems.

The ability to observe in vivo drug pharmacokinetics can be useful in identifying the responsiveness of different patient groups to specific pharmacologically active agents. For example, let us consider a presumed clinically homogeneous population of patients in which a specific drug is effective in alleviating symptoms in 15 percent. Such a therapy would be considered relatively ineffective for that population as a whole. However, for the 15 percent that responded, the therapy is quite effective. Conventional techniques may not be sensitive enough to identify subpopulations with specific pharmacological sensitivities to different agents. PET studies with either of the two strategies outlined above could provide additional diagnostic information that could potentially segregate such subgroups and allow for more specific and pathophysiologically appropriate therapies to be employed.

A number of labeled compounds have been developed for use with PET in the study of dopaminergic (*42*), opiate (*43*), benzodiazepine (*44*), and other systems (*45*) (Table 1). Labeled ligands of high specific activity have been shown with PET to reflect specific receptor systems as determined by their localization in appropriate anatomical sites, competitive blockade, and kinetic differentiation of specific and nonspecific binding in serial measurements (*42–45*) (Fig. 7). The use of appropriate positron-labeled compounds makes it possible to examine the presynaptic site of neurochemical transmission with a labeled precursor of an active agent such as ^{18}F-labeled L-dopa (*42*), or to examine postsynaptic receptor interactions with an agent such

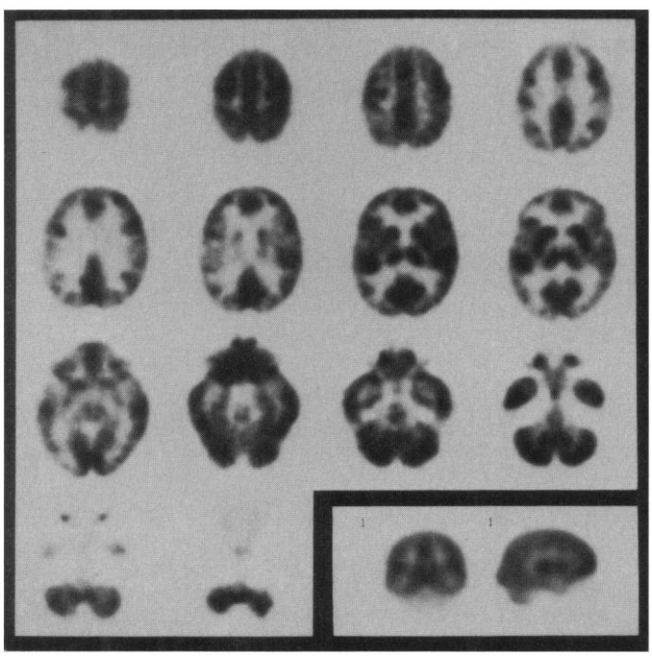

Fig. 8. Complete set of FDG-PET images from a normal subject, demonstrating glucose utilization. These images were obtained with an 8-mm interval between slices with the Neuro-ECAT system (image spatial resolution of 8.4 by 8.4 by 12.5 mm). The two images in the lower right corner are anterior-posterior and lateral two-dimensional views (rectilinear studies) of the same subject obtained prior to the tomographic examination. The PET device provides identification of the position of the tomographic planes and allows superimposition of their location on the rectilinear images. Shades of gray, units of micromoles per minute per milligram, with black representing the highest value. At this spatial resolution, the folds in the cortical ribbon are clearly delineated, as are the subcortical structures (right-most images, second row) including the thalamus, caudate, and the lenticular nuclei (putamen-globus pallidus complex). Both the posterior and the anterior limbs of the internal capsule are visualized. The hippocampus-parahippocampal gyri region can be seen lateral to the brain stem, along the medial portions of the temporal lobes (third row, extreme left). Substructures of the posterior fossa are visible (third row, extreme right) and include the brainstem and the substructures of the cerebellum (the cerebellar cortex, vermis, and dentate nuclei). This study demonstrates the progressive increase in image quality that has occurred as the spatial resolution of PET devices has improved. For example, compare the image quality and detail in Figs. 3, b and c, 4 and 5, obtained with a tomograph having a spatial resolution of 16 by 16 by 18 mm with those in this figure. Tomographs with 2- to 4-mm resolution are now being tested. Improvements in spatial resolution not only increase the anatomical detail, the structure identification capacity, and the quantitative accuracy. [From M. E. Phelps *et al.*, in (*3*); courtesy of *Journal of Cerebral Blood Flow and Metabolism*]

as ^{11}C-labeled *N*-methylspiperone (*42*), or ^{18}F-labeled spiperone (*42*) for the (D_2) dopamineric sites, or ^{11}C-labeled carfentanil (*43*) for the (mu) opiate sites (Fig. 7). To transform these types of studies into measurements of processes such as receptor affinity and density, neurotransmitter concentration and turnover, ligand on and off rates, and diffusion rates requires formulation and kinetic and biochemical verification of models, whether for PET or any in vivo estimation (*3, 46*).

Conclusion

The examples of the use of PET to examine structure-function relationships, physiological psychology, pharmacology, stoichiometry, and pathophysiology of disease illustrate some of the diverse types of investigational strategies that can be utilized with this technology. The further course of development of PET depends not only on advances in the technology itself (Fig. 8) but also on its role in using and applying advances from the basic biomedical sciences to human studies. This is aided by the many types of labeled compounds already available, or that can be synthesized, providing PET with a broad range of biochemical and physiological probes for examining different processes of the brain. Required advances in the number and validity of tracer kinetic models continue not only in the field of PET but in all those fields where radioactive labeled tracers are used. The importance of an analogous scientific method for studies in man to those in a laboratory setting, underscores the significance and potentials of PET.

References and Notes

1. M. E. Phelps, E. J. Hoffman, N. A. Mullani, M. M. Ter-Pogossian, *J. Nucl. Med.* **16**, 210 (1975).
2. M. E. Raichle, *Brain Res. Rev.* **1**, 47 (1979); M. M. Ter-Pogossian, M. E. Raichle, B. E. Sobel, *Sci. Am.* **243**, 170 (1980).
3. M. E. Phelps, J. C. Mazziotta, S. C. Huang, *J. Cereb. Blood Flow Metab.* **2**, 113 (1981); M. Walker, *Ann. Neurol.* **15** (suppl.), S1 (1984); W. D. Heiss and M. E. Phelps, *Positron Emission Tomography of the Brain* (Springer-Verlag, New York, 1983).
4. J. S. Fowler and A. P. Wolf, in *Nuclear Sciences Series*, NAS-NS-3201 (National Academy of Sciences–National Research Council, Washington, D.C., 1983); M. J. Welch and J. P. Tewson, in *Radiopharmaceuticals II*, J. A. Sorenson, Ed. (Society of Nuclear Medicine, New York, 1979), pp. 201.
5. L. Sokoloff *et al.*, *J. Neurochem.* **18**, 897 (1979); L. Sokoloff, *J. Cereb. Blood Flow Metab.* **1**, 7 (1981); *Ann. Neurol.* **15** (suppl), S1 (1984).
6. E. M. Bessell, A. B. Foster, J. H. Westwood, *Biochem. J.* **128**, 199 (1972); B. M. Gallagher *et al.*, *J. Nucl. Med.* **19**, 1154 (1978); E. E. Machado de Domenech and A. Sols, *FEBS Lett.* **119**, 174 (1980).
7. M. E. Phelps *et al.*, *Ann. Neurol* **6**, 371 (1979); S. C. Huang *et al.*, *Am. J. Physiol.* **238**, E69 (1980).
8. M. Reivich *et al.*, *Circ. Res.* **44**, 127 (1979).
9. R. Hawkins, M. E. Phelps, S. C. Huang, D. E. Kuhl, *J. Cereb. Blood Flow Metab.* **1**, 37 (1981).
10. F. Schuier *et al.*, *ibid.* **1** (suppl. 1), S63 (1981).
10a. B. K. Siesjo, personal communication.
11. M. E. Phelps, S. C. Huang, J. C. Mazziotta, R. A. Hawkins, *J. Cereb. Blood Flow Metab.* **3** (suppl. 1), S131 (1983); A. Gjedde and N. H. Diemer, *ibid.*, p. 303; W. M. Pardridge *et al.*, *ibid.* **2**, 197 (1982).
12. S. S. Kety, *Pharmacol. Rev.* **3**, 1 (1951).
13. B. K. Siesjo, *Brain Energy Metabolism* (Wiley, New York, 1978), p. 101.
14. R. A. Hawkins, W. K. Hass, J. Ransohoff, *Stroke* **10**, 690 (1979).
15. M. E. Raichle *et al.*, *Am. J. Physiol.* **228**, 1936 (1975).
16. R. H. Ackerman *et al.*, *Arch. Neurol.* **38**, 537 (1981).
17. J. Engel, Jr., D. E. Kuhl, M. E. Phelps, J. C. Mazziotta, *Ann. Neurol.* **12**, 510 (1982); D. E. Kuhl, J. Engel, Jr., M. E. Phelps, C. Selin, *ibid.* **8**, 348 (1980); J. C. Mazziotta and J. Engel, Jr., *Epilepsia* **25** (suppl. 2), S86 (1984); W. H. Theodore *et al.*, *Ann. Neurol.* **14**, 419 (1983).
18. J. Engel, Jr., D. E. Kuhl, M. E. Phelps, R. Rausch, M. Nuwer, *Neurology* **33**, 400 (1983).
19. J. Engel, Jr., D. E. Kuhl, M. E. Phelps, *Science* **218**, 64 (1982).
20. R. F. Ackermann, D. M. Finch, T. L. Babb, J. Engel, Jr., *J. Neurosci.* **4**, 251 (1984); Y. Ben Ari, E. Tremblay, D. Riche, E. Ghilini, R. Naquet, *Neuroscience* **6**, 1361 (1981); W. F. Caveness *et al.*, *Ann. Neurol.* **7**, 213 (1980); R. C. Collins, *Brain Res.* **150**, 487 (1978); R. E. Watson *et al.*, *Brain Res. Rev.* **5**, 133 (1983).
21. S. Bernardi, M. R. Trimble, R. S. Frackowiak, R. J. Wise, T. Jones, *J. Neurol. Neurosurg. Psychiatr.* **46**, 473 (1983).
22. M. E. Phelps, J. C. Mazziotta, L. Baxter, R. Gerner, *Ann. Neurol.* **15** (suppl.), S192 (1984); L. R. Baxter *et al.*, *Arch. Gen. Psychiatr.* **42**, 1985.
23. W. Penfield and T. Rasmussen, *The Cerebral Cortex of Man* (Macmillan, New York, 1950).
24. J. Greenberg *et al.*, *Science* **212**, 678 (1981); M. Kushner *et al.*, *Ann. Neurol.* **12**, 89 (1982); J. C. Mazziotta, M. E. Phelps, E. Halgren, *Human Neurobiol.* **2**, 11 (1983); J. C. Mazziotta *et al.*, *J. Cereb. Blood Flow Metab.* **3** (suppl. 1), S246 (1983); M. Reivich *et al.*, *Acta Neurol. Scand.* **60** (suppl. 72), 198 (1979); E. L. Schwartz, D. R. Christman, A. P. Wolf, *Brain Res.* **294**, 225 (1984).
25. M. E. Phelps, D. E. Kuhl, J. C. Mazziotta, *Science* **211**, 1445 (1981).
26. M. E. Phelps *et al.*, *Neurology* **31**, 517 (1981).
27. P. T. Fox and M. E. Raichle, *J. Neurophysiology* **51**, 1109 (1984).
28. M. Reivich *et al.*, *J. Cereb. Blood Flow Metab.* **1** (suppl. 1), S471 (1981).
29. J. C. Mazziotta, M. E. Phelps, R. E. Carson, D. E. Kuhl, *Neurology* **32**, 921 (1982).
30. J. C. Mazziotta and M. E. Phelps, *Ann. Neurol.* **15** (suppl.), S50 (1984).
31. D. E. Kuhl *et al.*, *ibid.* **12**, 425 (1982); D. E. Kuhl *et al.*, *Brain Imaging and Brain Function* (Raven, New York, in press).
32. J. Gusella *et al.*, *Nature (London)* **306**, 234 (1983).
33. R. H. Ackerman *et al.*, *J. Cereb. Blood Flow Metab.* **1** (suppl. 1), S502 (1981); J. C. Baron *et al.*, *Trans. Amer. Neurol. Ass.* **105**, 459 (1980); J. C. Baron *et al.*, *Acta Neurol. Scand.* **60** (suppl. 72), 324 (1979); G. L. Lenzi *et al.*, *Eur. Neurol.* **20**, 285 (1981); W. R. Martin and M. E. Raichle, *Ann. Neurol.* **14**, 168 (1983).
34. J. C. Baron, M. G. Bousser, D. Comar, F. Sousaline, P. Castaigne, *Eur. Neurol.* **20**, 273 (1981); R. S. Frackowiak and R. J. Wise, *Neurol. Clin.* **1**, 183 (1983); R. J. Wise, S. Bernardi, R. S. Frackowiak, N. J. Legg, T. Jones, *Brain* **106**, 197 (1983); R. J. Wise, *Ann. Neurol.* **14**, 627 (1983); R. S. Frackowiak *et al.*, *J. Comput. Assist. Tomogr.* **4**, 727 (1980).
35. G. L. Lenzi, R. S. Frackowiak, T. Jones, *J. Cereb. Blood Flow Metab.* **1**, (suppl. 1), S504 (1981).
36. J. C. Baron *et al.*, *Stroke* **12**, 454 (1981).
37. J. M. Gibbs *et al.*, *J. Cereb. Blood Flow Metab.* **3** (suppl. 1), S590 (1983); W. R. Martin *et al.*, *Neurology* **32** (suppl. 2), A89 (1982); W. J. Powers, W. R. Martin, P. Herscovitch, M. E. Raichle, R. Grubb, *J. Nucl. Med.* **24**, P108 (1983); Y. L. Yamamoto, S. Little, C. Thompson, E. Meyers, I. V. Feindel, *Acta Neurol. Scand.* **60** (suppl. 72), 522 (1979).
38. M. Bergstrom, *J. Comput. Assist. Tomogr.* **7**, 1062 (1983); M. Ito *et al.*, *Neuroradiology* **23**, 63 (1982); C. G. Rhodes *et al.*, *Ann. Neurol.* **14**, 614 (1983).
39. G. DiChiro *et al.*, *J. Cereb. Blood Flow Metab.* **1** (suppl. 1), S11 (1981); G. DiChiro *et al.*, *Neurology* **32**, 1323 (1982); G. DiChiro *et al.*, in *Positron Emission Tomography of the Brain*, W. D. Heiss and M. E. Phelps, Eds. (Springer-Verlag, New York, 1983), p. 182; G. DiChiro *et al.*, *J. Comput. Assist. Tomogr.* **7**, 937 (1983); P. L. Kornblith *et al.*, in *Progress in Experimental Brain Tumor Research*, M. L. Rosenblum and C. B. Wilson, Eds. (Karger, Basel, in press).
40. N. J. Patronas *et al.*, *Radiology* **144**, 885 (1982).
41. M. E. Phelps, J. C. Mazziotta, R. Gerner, L. Baxter, D. E. Kuhl, *J. Cereb. Blood Flow Metab.* **3** (suppl. 1), S7 (1983); J. McCulloch, in *Handbook of Psychopharmacology*, L. L. Iverson, S. D. Iverson, S. H. Snyder, Eds. (Plenum, New York, 1982), p. 321.
42. E. S. Garnett, G. Firnau, C. Nahmias, *Nature (London)* **305**, 137 (1983); K. L. Leenders *et al.*, *Lancet* **1984-II**, 110 (1984); J. C. Baron *et al.*, in *Positron Emission Tomography of the Brain*, W. D. Heiss and M. E. Phelps, Eds. (Springer-Verlag, New York, 1983), p. 212; H. N. Wagner, Jr., *et al.*, *Science* **221**, 1264 (1983).
43. M. Maziere *et al.*, *J. Labeled Compd. Radiopharmacol.* **18**, 15 (1981); J. J. Frost *et al.*, *J. Nucl. Med.* **25**, P73 (1984).
44. D. Comar, M. Maziere, J. M. Gadot, G. Berger, F. Sousalline, *Nature (London)* **280**, 3291 (1979).
45. J. C. Baron, *Neurology* **33**, 580 (1983).
46. M. A. Mintun, M. E. Raichle, M. R. Kilbourne, G. F. Wooten, M. J. Welch, *Ann. Neurol.* **15**, 217 (1984).
47. D. E. Kuhl, *Radiology* **150**, 625 (1984).

48. In normal brain about 5.6 mol of oxygen are used per mole of glucose. PET measurements of oxygen and glucose utilization allow calculations of this ratio in patient studies. The tumor in Fig. 6a (arrow) has a significant reduction in this ratio (value of about 1.9) indicating its dependence on anaerobic glycolysis despite adequate oxygen availability through its elevated blood flow. Although there is depressed function of the cortex on the right in this patient, the molar ratio of oxygen to glucose is normal (about 5.4), an indication that this is unlikely to be a result of ischemia from pressure effects or direct tumor infiltration of the cortex. Rather, this change most likely represents a functional drop in neuronal activity due to disruption of fiber tracts (as was seen in Fig. 1). This type of information (blood flow, anaerobic or aerobic status) is an important factor in planning radio- or chemotherapy of neoplastic lesions.

49. We thank the many investigators who contributed their time and data to this article, Ron Sumida for technical assistance, and Lee Griswold for preparing illustrations. Supported in part by DOE contract AMO3-76-SF00012, NIH grants RO1-6M-248389, PO1-NS-15654, NIMH grant RO1-MH-37916-02, grants from the Hereditary Disease and Wills Foundations, donations from the Jennifer Jones Simon Foundation, and NINCDS (J.C.M.) Teacher-Investigator Award 1K07-00588-04-NSPA.